

# Diffusion behavior of water confined in deformed carbon nanotubes

Bruno H. S. Mendonça<sup>a,b,\*</sup>, Débora N. de Freitas<sup>b,c</sup>, Mateus H. Köhler<sup>a</sup>,  
Ronaldo J. C. Batista<sup>b</sup>, Marcia C. Barbosa<sup>a</sup>, Alan B. de Oliveira<sup>b</sup>

<sup>a</sup>*Instituto de Física, Universidade Federal do Rio Grande do Sul, Porto Alegre, RS  
91501-970, Brazil*

<sup>b</sup>*Departamento de Física, Universidade Federal de Ouro Preto, Ouro Preto, MG  
35400-000, Brazil*

<sup>c</sup>*Departamento de Física, Universidade Federal de Juiz de Fora, Juiz de Fora, MG  
36036-330, Brazil*

---

## Abstract

We use molecular dynamics simulations to study the diffusion of water inside deformed carbon nanotubes with different degrees of eccentricity at 300K. We found a water structural transition between tubular-like to single-file for (7,7) nanotubes associated with change from a high to low mobility regimes. Water is frozen when confined in a perfect (9,9) nanotube and it becomes liquid if such a nanotube is deformed above a certain threshold. Water diffusion enhancement (suppression) is related to a reduction (increase) in the number of hydrogen bonds. This suggests that the shape of the nanotube is an important ingredient when considering the dynamical and structural properties of confined water.

*Keywords:* Confined Water; Mobility; Carbon Nanotube; Diffusion.

---

## 1. Introduction

Fluids under nanoscale confinement exhibit properties not observed in the bulk [1, 2]. In the case of water this shows an even larger impact. When confined in carbon nanotubes (CNTs) water exhibits flow rates which exceeds

---

\*Corresponding author.

*Email address:* brunnohenrique13@gmail.com (Bruno H. S. Mendonça)

by three orders of magnitude the values predicted by the continuum hydrodynamic theory [3–12]. The superflow is not the only anomalous behavior observed in nanoconfined water. It also presents multi-phase flow, structural transitions and highly heterogeneous hydrogen bonds distribution [13–15].

For instance, the water diffusion coefficient in pristine carbon nanotubes does not decrease monotonically with the diameter of the tube [16]. Instead, it has a minimum for the (9,9) CNT, a maximum for the (20,20) nanotube and it approaches the bulk value for larger tubes. The nanoconfined water forms layers and molecules near the wall diffuse faster than the particles in the middle of the tube. This higher mobility is caused by dangling hydrogen bonds at the water-wall interface.

Although pristine nanotubes pose as perfect models for studying the confined water superflux [16], experimentally it is common to obtain nanotubes with defects, vacancies and structural distortions [17, 18]. In addition functional groups may be adsorbed onto tube’s surface, deposited at its entrance or even incorporated under compression. All these factors lead to structural deformations [19, 20], which in turn can affect the anomalous properties of the confined water. For example, the water streaming velocity and flow rate depend on the tube flexibility [21] and the effective shear stress and viscosity depend on the nanotube roughness, which affects more smaller tubes [22]. These observations were also supported by experiments revealing radius-dependent surface slippage in carbon nanotubes [23], and by simulations relating the shape of the nanotube with the dynamics of confined water with high influence on its flow and structure [24].

Carbon nanotubes have been speculated to be present in virtually all areas of life and physical sciences in a near future. From drug delivery to water desalination, the existent literature is vast. More specifically, several applications in nanofluidics have been explored. Examples include carbon nanotubes as nanosyringes [25] and nanothermometers [26]. Studies focusing fluid transport in carbon nanotubes are ubiquitous, with interest in possible practical applications and also in water properties itself, when confined in such a peculiar media [27–30].

In the real world carbon nanotubes are in the presence of substances, not only in its surroundings but filled with them. The contact between carbon nanotubes and substrates and/or surrounding adsorbates certainly change their structure. In this sense, the purpose of our work is to understand how deformations in carbon nanotubes change the diffusion of the confined water. Considering the majority of literature regarding water diffusion in

carbon nanotubes approach the problem using perfect nanotubes, we believe our work may fill a small piece of this important puzzle.

Here we explore in a systematic way by computer simulations the effect of the change in the eccentricity of the nanotube on the behavior of the diffusion coefficient for different nanotube diameters. The idea behind this work is to explore if there is a threshold distortion limit beyond which the diffusion is non anomalous. This means that it would decrease with the diameter of the nanotube as in normal, non water-like fluids.

The paper is organised as follows. We present details of simulations in Sec. 2, in Sec. 3 we discuss the results and the Sec. 4 ends the paper with our conclusions.

## 2. Computational Details and Methods

We performed molecular dynamics (MD) simulations for the TIP4P/2005 water model [31] using the LAMMPS package [32]. The SHAKE algorithm [33] was used to keep water molecules structure. The choice of TIP4P/2005 over many other models available in literature was due to its accuracy in calculating water transport properties at ambient conditions [34]. We represented the non-bonded interactions (carbon-oxygen) by the Lennard-Jones (LJ) potential with parameters  $\epsilon_{CO} = 0.11831$  kcal/mol and  $\sigma_{CO} = 3.28$  Å [27]. Interaction between carbon and hydrogen was set to zero. LJ cutoff distance was 12 Å and long-range Coulomb interactions were treated using the particle–particle particle–mesh method. [35] The time step used was 1 fs. The nanotubes considered were armchair with index  $n = 7, 9, 12, 16, 20,$  and 40.

During carbon nanotubes deformation process, carbon-carbon interaction was modelled via AIREBO potential [36, 37]. After reaching the desired degree of deformation, nanotubes were frozen, i.e., carbon atoms neither interact nor move relative to each other.

Nanotubes filling process goes as follows. First, water reservoirs containing a total of 8.000 water molecules were connected to both nanotubes ends as shown in Figure 1(a). Pressure and temperature of reservoirs were kept at 1 atm and 300 K, respectively, by means of Nosé-Hoover barostat and thermostat. After a few nanoseconds the equilibrium configuration in which nanotubes are filled with water is reached as depicted in Figure 1(b). Next, the reservoirs are removed and the simulation box size is adjusted to fit the nanotubes length as shown in Figure 1(c). Boundary conditions were periodic

in all directions during all stages. The number of water molecules enclosed depend on nanotubes dimensions. This information can be found in Table 1.

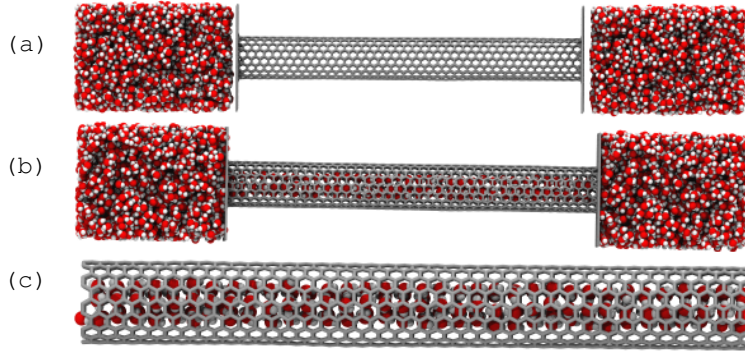


Figure 1: The three main steps for filling nanotubes with water are as follows. (a) Undeformed carbon nanotubes are placed between water reservoirs at 300 K and 1 atm. (b) After a few nanoseconds they become completely filled with water. (c) The reservoirs are removed and the nanotubes are made periodic in the axial direction.

Table 1: Carbon nanotubes diameter  $d$ , length  $L_z$ , and number of water molecules inside.

CNT (n,n)	$d$ (nm)	$L_z$ (nm)	Number of $H_2O$
(7,7)	0.95	123.4	901
(9,9)	1.22	50.66	908
(12,12)	1.62	22.62	901
(16,16)	2.17	11.06	911
(20,20)	2.71	10.33	1440
(40,40)	5.42	7.87	5221

After perfect nanotubes are filled with water, they are compressed to different degrees of deformation by loading them with plates made of frozen atoms (see Figure 2). The interaction between CNTs and plates was given by the repulsive part of LJ potential with energy parameter  $\epsilon = 0.184$  kcal/mol and distance parameter  $\sigma = 3.0$  Å. The cutoff used was 3.0 Å. For compressing the nanotubes plates are approached to each other at constant speed until the nanotube reaches the desired deformation. Speeds were in the range from 0.2 to 0.6 Å/ps.

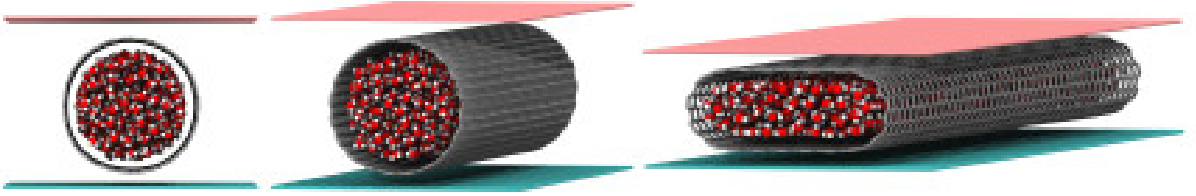


Figure 2: Carbon nanotube between parallel plates.

Nanotubes deformation are characterised by eccentricity after compression, which reads

$$e = \sqrt{1 - \frac{b^2}{a^2}}, \quad (1)$$

where  $b$  and  $a$  being the smaller and larger semi-axis, respectively. We approached nanotubes with eccentricities ranging from 0.0 (perfect) to 0.8 (highly deformed) as shown in Figure 3.

Then, long simulations of water inside deformed carbon nanotubes were carried out for nanotubes with different diameters. The production part was conducted in the canonical ensemble, with temperature fixed at 300 K using the Nosé-Hoover thermostat [38] with a time constant of 0.1 ps. After filling and deforming nanotubes, the system was allowed to equilibrate for 5 ns before data collection.

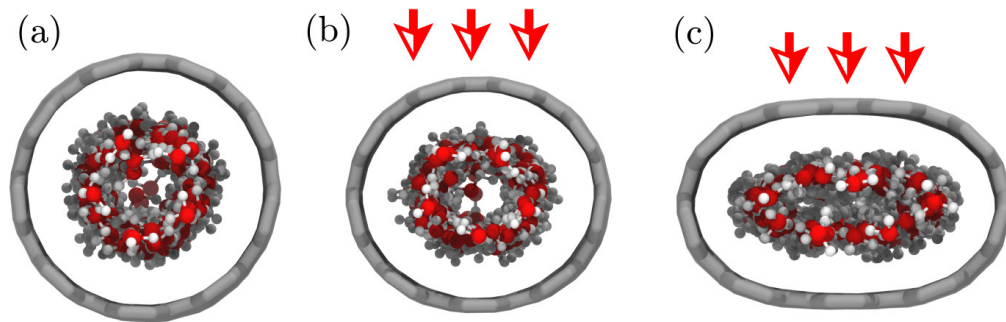


Figure 3: Snapshots of the (9,9) CNT at (a)  $e = 0.0$ , (b)  $e = 0.4$ , and (c)  $e = 0.8$ .

To study the mobility we employed the mean squared displacement (MSD) given by: [39]

$$\langle \Delta \vec{r}(t)^2 \rangle = \langle |\vec{r}(t) - \vec{r}(0)|^2 \rangle \quad (2)$$

where  $\langle |\vec{r}(t) - \vec{r}(0)|^2 \rangle$  is referred as the MSD,  $\langle \rangle$  denotes an average over all molecules and  $\vec{r}(t)$  is the displacement of a molecule during the time interval  $t$ . Diffusion constant  $D$  is related to MSD and time through the relation

$$\langle \Delta \vec{r}(t)^2 \rangle \propto Dt^\alpha, \quad (3)$$

where  $\alpha$  is a signature of which type of diffusive regime the system is following namely  $\alpha = 1$  is the Fickian diffusion,  $\alpha > 1$  indicates the superdiffusive regime and  $\alpha < 1$  refers to the sub-diffusive regime. In the bulk phase, water molecules obey Fickian diffusion. When confined in CNTs the diffusion of water molecules becomes more involving due to the nanoscale confinement. [39]

For the hydrogen bonds statistics we used the geometrical criteria of donor-hydrogen-acceptor (DHA) angle and donor-acceptor (DA) distance. A hydrogen bond is computed if DHA angle  $\leq 30^\circ$  and DA distance  $< 0.35$  nm [40, 41].

### 3. Results

In Figure 4 we show the diffusion coefficient of water as a function of the diameter for the perfect nanotube ( $e = 0$ ) for the TIP4P/2005 water model (both from this work and from Köhler et al. [42]) and for the SPC/E water from Ref. [16]. For the two models, the diffusion coefficient shows a global minimum at 1 nm diameter which corresponds to a (9,9) CNT. In this case the mobility of molecules is virtually zero. The water is frozen inside the nanotube assuming a solid ring-like structure, as can be seen in Figure 6(c). This ring is immobile and each molecule makes a large number of hydrogen bonds as shown in Figure 7. The low dynamics seen in water confined in (9,9) CNT is due to the commensurability with the hydrogen bonds distance and (9,9) CNT diameter, which favours the formation of an organised network as Figure 6 illustrates. The interplay between the diffusion coefficient showed in Figure 6 and the hydrogen bonds network illustrated in Figure 7 is the mechanism behind the anomalous behaviour of confined water [16, 42].

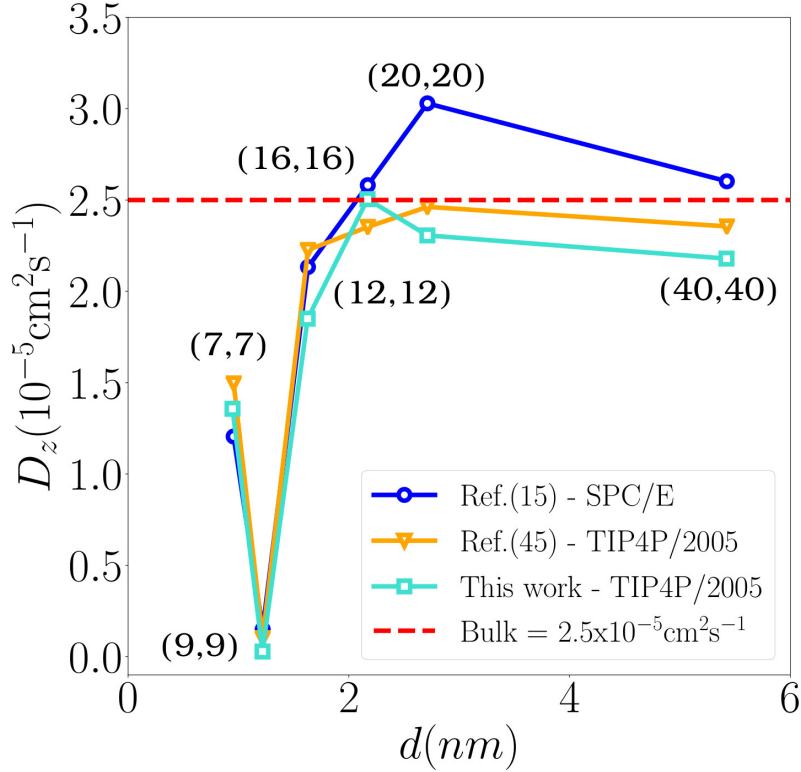


Figure 4: Diffusion coefficient versus diameter of the carbon nanotube for the perfect  $e = 0$  tube .

For larger nanotube diameters the diffusion coefficient approaches the bulk value (around  $2.5 \times 10^{-5} \text{ cm}^2/\text{s}$ ) [43]. For intermediate nanotube diameters (2-3 nm), there is a maximum in the diffusion coefficient. Larger surface areas induce more dangling bonds, while large central volumes favours hydrogen bonds formation. The minimum and maximum observed in the diffusion coefficient are related to this competition between the water-wall contact area and the volume occupied by the fluid [16].

In Eq. (3) we found  $\alpha = 1$ , which is a signature of Fickian diffusion. In Fig. 5 we show MSD curves as a function of time for carbon nanotubes with  $n = 7, 9, 12, 16$  and  $20$ , with eccentricities (a)  $e = 0.0$ , (b)  $e = 0.4$  and (c)  $e = 0.8$ .

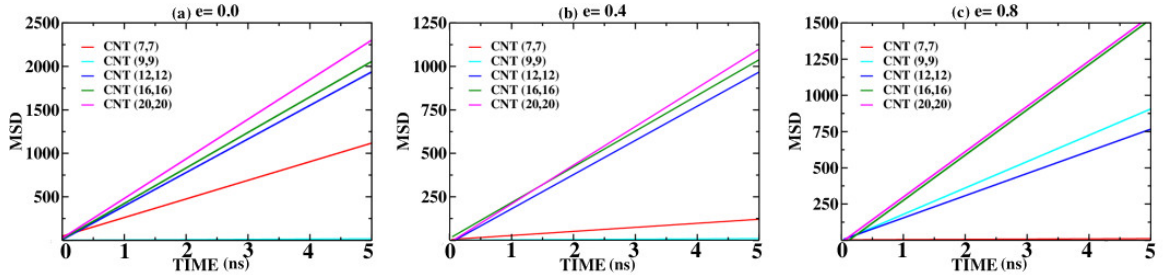


Figure 5: MSD curves as a function of time for the carbon nanotubes  $n=7, 9, 12, 16$  and  $20$  for (a)  $e = 0.0$ , (b)  $e = 0.4$  and (c)  $e = 0.8$ .

Figure 6 shows snapshots of the last simulation steps and the radial density maps for the nanotubes with  $e = 0.0$  (left) and  $e = 0.8$  (right). This Figure also shows the oxygen density maps constructed by dividing the nanotubes radial direction into small concentric bins and by averaging the number of oxygen atoms in each bin. Red regions represent high probability of finding a water molecule while dark blue stands for low probability. For the (7,7) nanotube, [Figure 6(a) and (b)] the increase in deformation makes water molecules to undergo a structural transition: from a cylindrical organisation to two single-file structures. Molecules in one single-file tend to bond to particles in the other single-file. Then, the deformation in (7,7) nanotubes leads to a high-mobility to low-mobility transition due to an increasing in the number of hydrogen bonds.



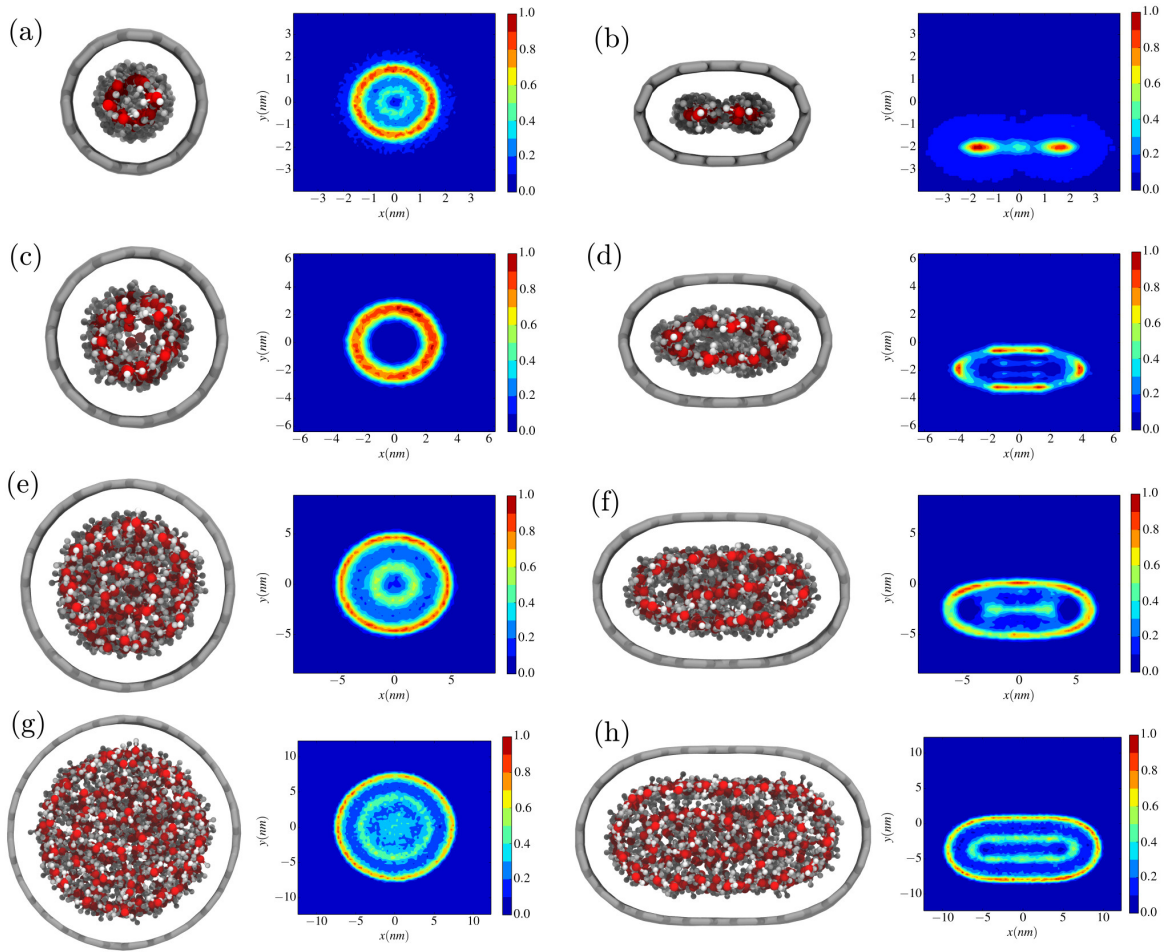


Figure 6: Left panels: snapshots of water molecules inside nanotubes along with radial ( $x$ - $y$ ) density maps of oxygens inside (a) (7,7), (c) (9,9), (e) (12,12) and (g) (16,16) carbon nanotubes with eccentricity  $e = 0.0$ . Right panels show the correspondent nanotubes with  $e = 0.8$ .

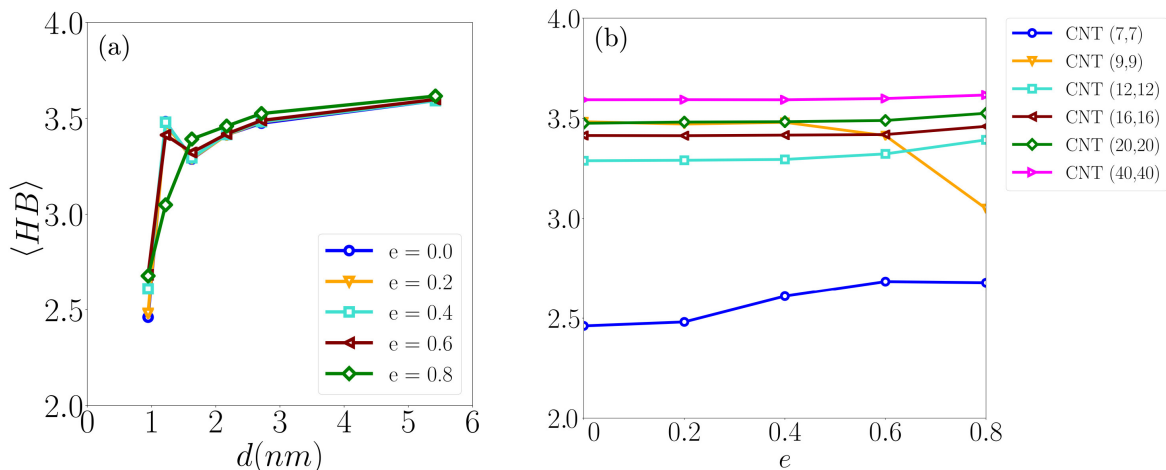


Figure 7: Average number of hydrogen bonds (HB) of each water molecule as a function of (a) the nanotube diameter relative of the nanotube  $e = 0.0$  and (b) the eccentricity.

For the (9,9) nanotube [Figure 6(c) and (d)] as the deformation is imposed we observe a transition from an uniform frozen water layer to non uniform liquid water layered structure. For  $e = 0.8$  clusters of fluid water at the wall replace the frozen  $e = 0.0$  structure. The deformation in the case (9,9) leads to low-mobility for a high-mobility transition.

For the larger tubes, (12,12) and (16,16), [Figures 6(e) to (h)] the systems form liquid layers, which despite deformed are preserved under tension. For (20,20) and (40,40) CNTs no representative transformation is observed as we increase the eccentricity.

In order to test if the structural transitions observed for the (7,7) and (9,9) nanotubes are related to changes in the mobility MSDs of confined water were computed. Figure 8(a) shows the diffusion coefficient of water as a function of the nanotube diameter  $d$  for different eccentricities ( $0 \leq e \leq 0.8$ ). For the highest deformations ( $e = 0.6$  and  $e = 0.8$ ) systems show no increase in  $D$  for diameters below 1.5 nm as observed for the undeformed case. This suggests that the deformation suppresses the anomalous high diffusion (and maybe flux) observed in confined water.

Figure 8(b) illustrates the change in the water diffusion coefficient with deformation  $e$ . For the (7,7) case the increase of  $e$  leads to a decrease in the diffusion coefficient, which is related to the structural change observed in the Figure 6. This result indicates that any amount of deformation destroys the super diffusion observed in confined water. For the (9,9) case, the opposite

happens. As the deformation goes beyond a certain threshold, the water frozen at the wall melts. However in this case the transition requires a huge deformation.

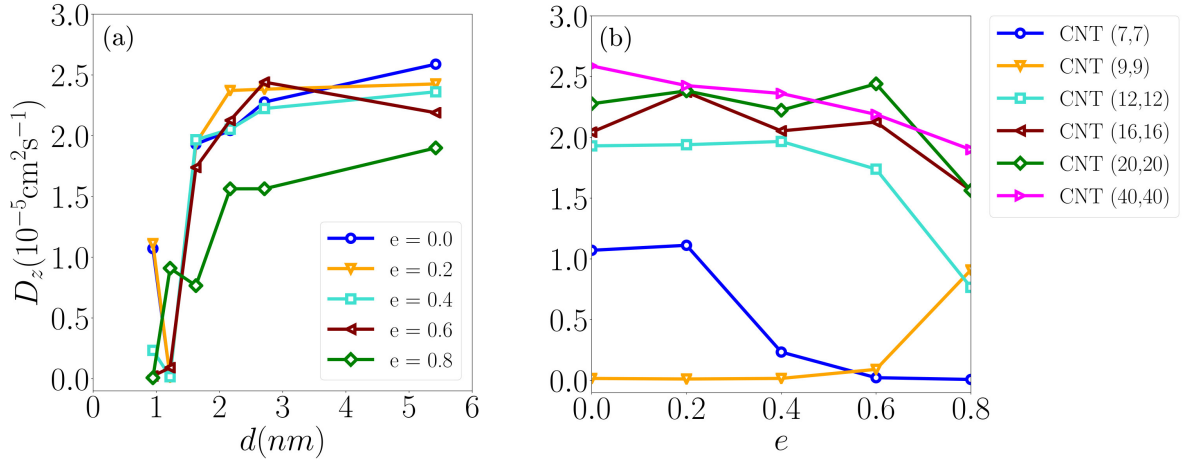


Figure 8: Axial diffusion coefficient of water as a function of (a) the diameter relative of the nanotube  $e = 0.0$  and (b) eccentricity.

For understanding the relation between dynamics and structure assumed by the confined water, we calculated the average number of hydrogen bonds of each molecule for the different systems studied. Figure. 7(a) shows that this number is highly dependent on the nanotube size and tends to the bulk value for the larger nanotubes. For the  $e < 0.8$  a local maximum in the number of bonds occur at the (9,9) nanotube coinciding with the minimum of diffusion. For the  $e = 0.8$  no maximum in the number of bonds is observed what is agreement with the non zero diffusion and with our suggestion that the (9,9) system does not melt for the high deformation.

Figure 7 (b) illustrates the average number of hydrogen bonds of each water molecule as a function of the nanotube eccentricity. For the the (7,7) nanotube the water shows monotonically increase of hydrogen bonds what supports the idea that the decrease in the mobility with deformation is followed by the formation of a more bonded system. For the (9,9) CNT, the reduction of the number of hydrogen bonds at  $e = 0.8$  what supports the absence of melting in this case.

In order to confirm the correlation between the behaviour of the mobility and the number of hydrogen bonds we compute the percentual change of each of these quantities as follows. For each nanotube size the diffusion and

number of hydrogen bonds is renormalised by its maximum value. Figure 9 illustrates the percentage of the diffusion and of the number of bonds  $D/D_{max}$  and  $\langle HB \rangle / \langle HB \rangle_{max}$  as a function of the eccentricity. This figure confirms that diffusion correlates with the number of hydrogen bonds. For the (7,7), (12,12), (16,16), (20,20) and (40,40) the percentage diffusion decreases and the percentage number of bonds decrease with the increase of the eccentricity while for the (9,9) case the system is frozen for  $e \leq 0.6$ . This implies that the melting transition when the system changes from (9,9) to (7,7) is suppressed by the high eccentricity.

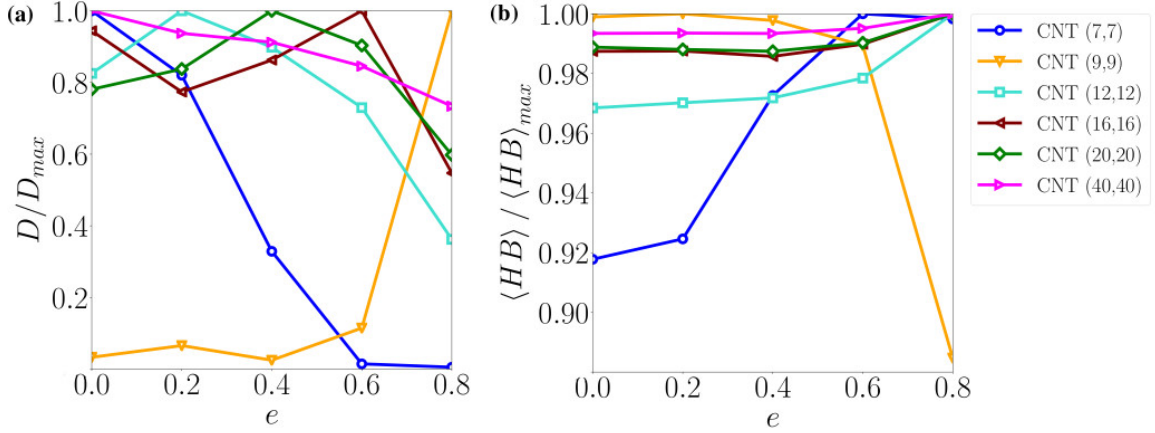


Figure 9: Percentage fraction (a)  $D/D_{max}$  and (b)  $\langle HB \rangle / \langle HB \rangle_{max}$  per water molecule as a function of the nanotube eccentricity.

#### 4. Conclusion

We investigated the effect of deforming CNTs in the structure and diffusion of the confined water.

We show that the deformation of the nanotube suppresses two phenomena observed in the diffusion of confined water: the increase of the diffusion with the decrease of the nanotube diameter and the freezing of confined water above the melting transition.

The disappearance of the diffusion enhancement is observed because the water at the (7,7) tube shows a smooth transition from a fluid to a frozen state as the tube is deformed. The suppression of the frozen state for the water at the (9,9) nanotube is observed by the increase of the water mobility at the deformation  $e = 0.8$ . In this case there is a critical diameter ( $\sim 1-1.2$

nm) for perfect nanotubes inside which the water freezes. By deforming the tube, varying the eccentricity  $e$  from 0 to 0.8, we have shown that inside this pores the hydrogen bonds break down and the crystalline structure is no longer favourable, leading to anomalous water diffusion. As we increase the nanotube diameter, the water diffusion presents a maximum in relation to the tube eccentricity, but at this point the effect of deformation is less prominent. This maximum is a consequence of the competition between nanotube area and water volume: the increase of the internal area of the tubes favours the break of hydrogen bonds in water (generating “dangling bonds”), while the increase in water volume favours the formation of hydrogen bonds.

For almost all systems, the increase in nanotube deformation leads to increase the number of hydrogen bonds, which slows down the water mobility. The only exception is the CNT (9,9) in which the deformation decreases the number of hydrogen bonds and increase the water diffusion. In this nanotube the symmetrical shape leads to frozen water molecules at interface, while the deformation leads to enhanced diffusion. All of these evidences point to the importance of the nanotube structure on the properties of the confined water.

## Acknowledgments

This work is partially supported by Brazilian agencies CNPq and CAPES, Universidade Federal de Ouro Preto, Universidade Federal do Rio Grande do Sul and INCT-Fcx. ABO thanks the Brazilian science agency FAPEMIG for financial support through the Pesquisador Mineiro grant. BHSM is indebted to Patricia Ternes who inspired the graphics of work.

## References

- [1] J. K. Holt, H. G. Park, Y. Wang, M. Stadermann, A. B. Artyukhin, C. P. Grigoropoulos, A. Noy, O. Bakajin, *Science* 312 (2006) 1034.
- [2] J. L. Bradley-Shaw, P. J. Camp, P. J. Dowding, K. Lewtas, *Langmuir* 32 (2016) 7707–7718.
- [3] M. Majumder, N. Chopra, R. Andrews, B. J. Hinds, *Nature* 438 (2005) 44.
- [4] G. Torrie, G. Lakatos, G. Patey, *The Journal of Chemical Physics* 133 (2010) 224703.

- [5] W. Nicholls, M. K. Borg, D. A. Lockerby, J. Reese, *Molecular Simulation* 38 (2012) 781–785.
- [6] K. Ritos, D. Mattia, F. Calabrò, J. M. Reese, *The Journal of Chemical Physics* 140 (2014) 014702.
- [7] L. Liu, G. Patey, *The Journal of Chemical Physics* 141 (2014) 18C518.
- [8] D. M. Holland, D. A. Lockerby, M. K. Borg, W. D. Nicholls, J. M. Reese, *Microfluidics and Nanofluidics* 18 (2015) 461–474.
- [9] K. Ritos, M. K. Borg, N. J. Mottram, J. M. Reese, *Philosophical Transactions of the Royal Society A* 374 (2016) 20150025.
- [10] L. Liu, G. Patey, *The Journal of Chemical Physics* 144 (2016) 184502.
- [11] M. K. Borg, J. M. Reese, *MRS Bulletin* 42 (2017) 294–299.
- [12] K. Ritos, M. K. Borg, D. A. Lockerby, D. R. Emerson, J. M. Reese, *Microfluidics and Nanofluidics* 19 (2015) 997–1010.
- [13] K. Nomura, T. Kaneko, J. Bai, J. S. Francisco, K. Yasuoka, X. C. Zeng, *Proceedings of the National Academy of Sciences* 114 (2017) 4066.
- [14] A. Barati Farimani, N. R. Aluru, *The Journal of Physical Chemistry C* 120 (2016) 23763.
- [15] P. Ternes, A. Mendoza-Coto, E. Salcedo, *The Journal of Chemical Physics* 147 (2017) 034510.
- [16] A. Barati Farimani, N. Aluru, *The Journal of Chemical Physics B* 115 (2011) 12145.
- [17] T. J. Sisto, L. N. Zakharov, B. M. White, R. Jasti, *Chemical Science* 7 (2016) 3681.
- [18] J. M. H. Kroes, F. Pietrucci, A. C. T. van Duin, W. Andreoni, *Journal of Chemical Theory and Computation* 11 (2015) 3393.
- [19] A. B. de Oliveira, H. Chacham, J. S. Soares, T. M. Manhabosco, H. F. de Resende, R. J. Batista, *Carbon* 96 (2016) 616.

- [20] Y. Umeno, T. Kitamura, A. Kushima, *Computational Materials Science* 30 (2004) 283.
- [21] A. Sam, S. K. Kannam, R. Hartkamp, S. P. Sathian, *The Journal of Chemical Physics* 146 (2017) 234701.
- [22] B. Xu, Y. Li, T. Park, , X. Chen, *The Journal of Chemical Physics* 135 (2011) 144703.
- [23] E. Secchi, S. Marbach, A. Nigues, D. Stein, A. Siria, L. Bocquet, *Nature* 537 (2016) 210.
- [24] C. Belin, L. Joly, F. Detcheverry, *Physical Review Fluids* 1 (2016) 054103.
- [25] J. K. Holt, A. Noy, T. Huser, D. Eaglesham, O. Bakajin, *Nano Letters* 4 (2004) 2245–2250.
- [26] Y. Gao, Y. Bando, *Nature* 415 (2002) 599.
- [27] G. Hummer, J. C. Rasaiah, J. P. Noworyta, *Nature* 414 (2001) 188.
- [28] M. Majumder, N. Chopra, R. Andrews, B. J. Hinds, *Nature* 438 (2005) 44.
- [29] I. Brovchenko, A. Geiger, A. Oleinikova, *Physical Chemistry Chemical Physics* 3 (2001) 1567–1569.
- [30] M. Whitby, N. Quirke, *Nature Nanotechnology* 2 (2007) 87.
- [31] J. L. F. Abascal, C. Vega, *The Journal of Chemical Physics* 123 (2005) 234505.
- [32] S. Plimpton, *Journal of Computational Physics* 117 (1995) 1.
- [33] J.-P. Ryckaert, G. Ciccotti, H. J. Berendsen, *Journal of Computational Physics* 23 (1977) 327.
- [34] M. Gonzalez, J. Abascal, *The Journal of Chemical Physics* 132 (2010) 096101.
- [35] R. W. Hockney, J. W. Eastwood, McGraw-Hill 1.

- [36] S. J. Stuart, A. B. Tutein, J. A. Harrison, *The Journal of Chemical Physics* 112 (2000) 6472.
- [37] D. W. Brenner, O. A. Shenderova, J. A. Harrison, S. J. Stuart, B. Ni, S. B. Sinnott, *Journal of Physics: Condensed Matter* 14 (2002) 783.
- [38] S. Nosé, *The Journal of Chemical Physics* 81 (1984) 511.
- [39] A. Striolo, *Nano Letters* 6 (2006) 633.
- [40] D. van der Spoel et al., *The Journal of Physical Chemistry B* 110 (2006) 4393.
- [41] S. Joseph, N. Aluru, *Nano Letters* 8 (2008) 452.
- [42] M. H. Köhler, L. B. da Silva, *Chemical Physics Letters* 645 (2016) 38.
- [43] K. R. Harris, L. A. Woolf, *The Journal of the Chemical Society, Faraday Transactions* 76 (1980) 377.